BIOMEDICAL ENGINEERING MSc PROGRAM
UNIVERSITY OF CRETE
TECHNICAL UNIVERSITY OF CRETE
FOUNDATION FOR RESEARCH AND TECHNOLOGY-HELLAS

Application Grade Thesis

Title:

"Biodegradable diblock and triblock copolymers for use in drug delivery"

Student's Name: Fergadis Georgios Dimitrios

Supervisor's Name: Prof. Maria Vamvakaki

2nd member committee name:

3rd member committee name:

Heraklion 2022

This dissertation is submitted as a partial fulfilment of the requirements for the Master's degree of Biomedical Engineering M.Sc. program

Acknowledgements

First of all, I would like thank my supervisor Professor Maria Vamvakaki for accepting me as a master's student in her lab and guided me through the whole process. Also I would like thank and express my gratitude to PhD candidate Maria Psarrou who helped me throughout the process by giving me advices, supporting me, evaluating my progress and being extremely patient with me. In addition, I couldn't left out my colleagues of the Synthetic Chemistry lab for all the help and support.

Last but not least I would like to thank my parents, Stamatis and Eleni as well as my brother Fotis for all the help and support I received throughout the years, from my undergraduate studies to my master's degree, and for providing me with all the essentials all the way through my life. I really could not thank them enough.

Abstract

Efficient drug delivery to the ocular tissues faces several challenges due to the presence of several dynamic and static barriers, such as the blood–ocular barrier, tear formation and the low permeability of the cornea. Several nanomedicines have been formulated and evaluated for ocular drug delivery over the years, among which are polymeric micelles, liposomes, hydrosizes, polymer-drug and protein-drug conjugates [1]. However, to the best of our knowledge, there are no examples of biodegradable systems, comprising materials which are approved by the Food and Drug Administration (FDA), being also capable of slowing down the release profile of drug, reported in the literature. Hence, the development of drug delivery systems that can ensure a suitable drug concentration for a prolonged time in different ocular tissues is certainly of great importance. In the present thesis, we aimed to develop polymeric nanocarriers for the encapsulation and delivery of Flurbiprofen, a nonsteroidal anti-inflammatory drug. Flurbiprofen is used before an ocular surgery in order to reduce or prevent miosis and it's also used orally for the symptomatic treatment of arthritis.

In the first part of this thesis, amphiphilic poly(ethylene glycol)-*block*-poly(L-lactide) (PEG-*b*-PLLA) diblock and PLLA-*b*-PEG-*b*-PLLA triblock copolymers were synthesized. For the polymer synthesis, the ring-opening polymerization of the hydrophobic monomer L-lactide was used [2]. Ring-opening polymerization (ROP) is a type of chain-growth polymerization in which the terminus of the polymer chain attacks the cyclic monomer to form longer polymer chains. The polymerization was carried out in the presence of stannous octoate ($Sn(Oct)_2$) as the catalyst. The successful synthesis of the polymers was verified by size exclusion chromatography (SEC) whereas their composition was determined by proton nuclear magnetic resonance (^{1}H NMR) spectroscopy.

In the second part of this thesis, the amphiphilic copolymers were self-assembled in water to form micellar structures, able to encapsulate small hydrophobic molecules [3]. The nanocarriers were prepared by dissolution of the polymer in an organic solvent followed by the dropwise addition of the aqueous phase. The size of the nanocarriers was determined by dynamic light scattering (DLS). The shape and the morphology of the nanocarriers was confirmed by scanning electron microscopy (SEM) and transmission electron microscopy (TEM), respectively.

Next, the release profile of Flurbiprofen from the polymeric nanocarriers was studied. Polymeric micelles from the diblock copolymer showed a release rate of 100% in four days of 8μg of Flurbiprofen, while micelles from the triblock copolymer had a release of 100% of 2.5μg of the drug at the same time. The more complex mixed micelles released 50% of the load in 6 hours and reached 100% release in 7 days, demonstrating a slower release rate compared to the diblock and triblock micelles.

Table of Contents

Chapter 1: Introduction

1.1. Drug delivery

Drug delivery systems (DDSs) are systems or devices that enable the introduction of a therapeutic substance in the body and improve its efficacy and safety by controlling the rate, time and site of release of the drug in the body [4]. The administration of these products can be achieved by oral, rectal or transnasal administration. In addition, widely used techniques include intravenous and subcutaneous injections. There is a constant evolution of the delivery methods in order to improve the effectiveness of administrated drugs. One aspect of the topic is related to the release rate of the drug. The sustained release of the pharmaceutical product can prolong its activity in the system and reduce the frequency of dosing [4]. A great deal of research has been also carried out, aiming to control the release of drug molecules by targeting specific organs or cells in the body [5],[6]. Nanocarriers such as liposomes, nanoparticles and micelles have been used for the sustained and targeted drug delivery of therapeutic agents [7], [8].

1.2. Ocular drug delivery

Efficient ocular drug delivery has been a great challenge for scientists due to the existence of unique anatomical and physiological barriers in the eye. These barriers include the tear film, the aqueous humor as well as the sclera, choroid and vitreous body. The barriers lead to fast drug elimination or low absorption from the eye, thus frequent administrations are required. The treatment for ocular diseases includes invasive and non-invasive methods (**Fig. 1.1**). Invasive treatments, like intraocular injections, surgery and laser therapy, are usually accompanied by complications, such as inflammation, high intraocular pressure, retinal hemorrhage and potential visual loss. Non-invasive therapies include oral medications, eye ointments and topical eye drops. Even though these methods have been widely used to treat various diseases, their sort life-time in the eye limit their clinical applications [6]. Recent developments in nanotechnology offer new opportunities to address the limitations of traditional drug delivery systems by developing nanostructures capable of encapsulating and transporting small molecules. Nanoparticles are defined as structures with sizes in the range of 1–1000 nm. The size of these particles should be less than 10 μm to avoid a foreign body

sensation after administration [9]. Potential candidates as drug carriers overcoming the problem of frequent administrations, are nanoparticles (NPs) comprising biodegradable polymers. The NPs can protect the drug from the proteins in the bloodstream, thereby increasing its half-life. They can also slow down the release profile of the drugs and as a result reduce the need for repeated dosing.

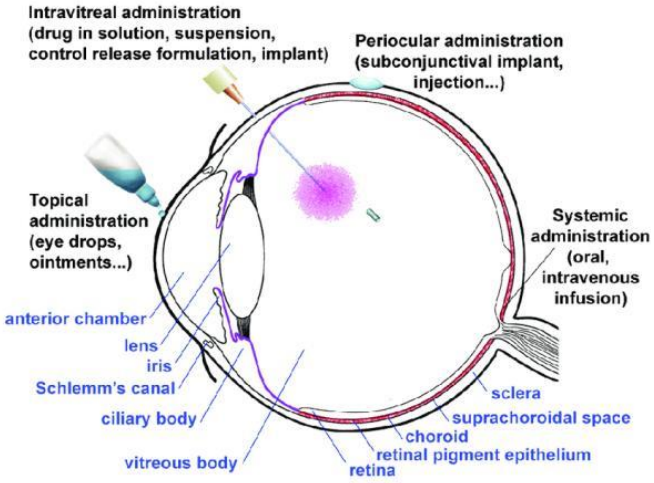

Fig. 1.1. The anatomy of the eye and various routes for drug administration. Adapted from ref. [10].

1.3. Types of nanocarriers

Since 1960, various nanocarriers have been extensively studied for the delivery of drugs. Liposomes, polymeric micelles, vesicles, polymer-drug conjugates are just some of them (**Fig. 1.2.**)

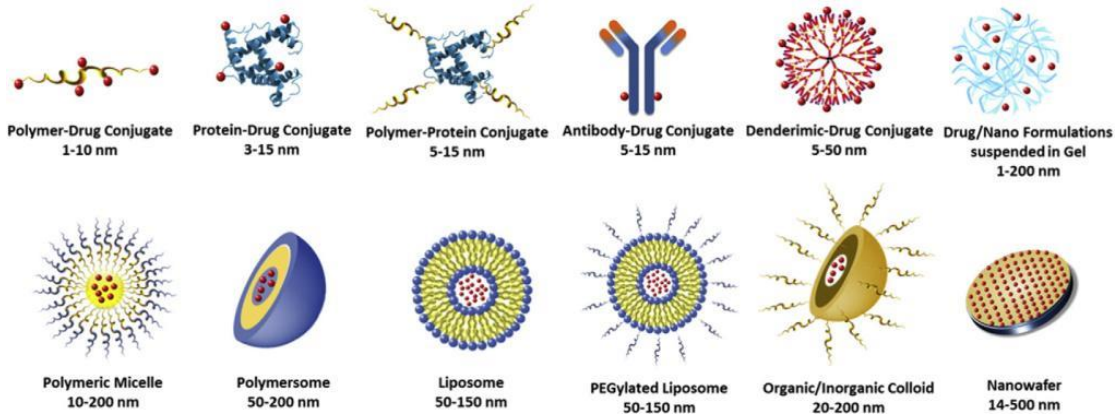

Fig. 1.2. Schematic depiction of the most relevant nanomedicine formulations for ocular delivery [1].

1.3.1. Liposomes

Liposomes are small "bubble-like" structures that have a phospholipid bilayer similar to a cell membrane and can hold hydrophilic or lipophilic medicines. Liposomes are the most common and well-studied drug delivery vehicles. In addition, poly(ethylene glycol) chains can be attached to the bilayer of liposomes to increase their circulation period in the bloodstream. Karn et al. found that liposomes containing cyclosporine A (CsA), a medication used to treat dry eye syndrome, cause less eye irritation and are more effective than commercial goods [11].

1.3.2. Polymeric nanoparticles

Polymeric nanoparticles (NPs) have a number of advantages over liposomes, including improved stability and the capacity to enable long-term drug release. Poly(lactic-co-glycolic acid) (PLGA) is a copolymer comprising poly(lactic acid) (PLA) and poly(glycolic acid) (PGA) that is commonly utilized in biomedical applications such surgical sutures, tissue engineering scaffolds, and drug delivery systems [12]. PLGA is an FDA-approved polymer that is biodegradable and can have its mechanical qualities altered by changing the PLA/PGA ratio and molecular weight. PLGA NPs can target specific regions or cells [13] and can encapsulate a variety of drugs [14]. *Cañadas et al* investigated the efficacy of PLGA NPs as a pranoprofen delivery mechanism within the cornea. Nanoparticles encapsulating pranoprofen had a rapid anti-inflammatory effect and a lengthy retention time on the cornea's surface, lowering ocular edema significantly [15]. Chitosan-based nanoparticles are another example.

Chitosan is a polysaccharide made by the deacetylation of chitin produced from crustacean shells. It contains glucosamine and N-acetylglucosamine units. Because of its mucoadhesive characteristics, chitosan has a high penetration of the ocular surface in ophthalmic drug administration [16]. Previous research has looked into the possibility of using chitosan-based NPs for ocular drug delivery [17],[18].

1.3.3. Polymeric micelles

Micelles are spherical structures formed by amphiphilic molecules self-assembling in a suitable solvent. Hydrophobic interactions cause amphiphilic molecules to self-assemble in an aqueous environment at a particular concentration, known as the critical micelle concentration (CMC) (**Fig. 1.3**). CMC stands for the minimum molecule concentration required for micelles to form. These structures have a hydrophobic core and a hydrophilic shell, and their size is typically in the nanometer range [19]. Amphiphilic diblock copolymers can self-assemble into polymeric micelles, with the hydrophobic blocks forming the inner core and the hydrophilic chains expanding in water to create the micelles' corona or shell [3].

Poly(ethylene glycol)-poly(propylene glycol) (PEG-PPG) [20], [21], poly(ethylene glycol)-poly(-caprolactone) (PEG-PCL) [22],[23], and poly(ethylene glycol)-poly(L-lactide) are among the most thoroughly investigated biodegradable block copolymers that may self-assemble into polymer micelles (PEG-PLLA). PLLA is a low-degradation synthetic hydrophobic polyester that has been properly modified to yield an amphiphilic polymer [24]. To make PEG-PLLA and PLLA-PEG-PLLA diblock copolymers, one alternative is to employ hydrophilic and biocompatible PEG chains [2], [25]. Polymeric chains can self-assemble into micellar nanostructures in an aqueous solution. These micelles are made up of a hydrophobic core comprised of PLLA blocks and a hydrophilic shell formed by PEG blocks. The core can serve as a reservoir for lipophilic drugs, whereas the shell stabilizes the micelles in the medium [5]. PEG-PLLA diblock and triblock copolymers have been investigated for use in drug delivery and tissue engineering [5],[26],[27].

There are two major ways for inducing the creation of polymer micelles. The non-selective-selective solvent approach involves dissolving the copolymer in a good solvent for both blocks, then adding water as a selective solvent to the solution. Micelles with a consistent size and low polydispersity are formed using this procedure. The polymer is dissolved in an organic solvent and then evaporated to create a polymer film in the second process. The polymer nanostructures are then formed once the film is hydrated with an aqueous solvent.

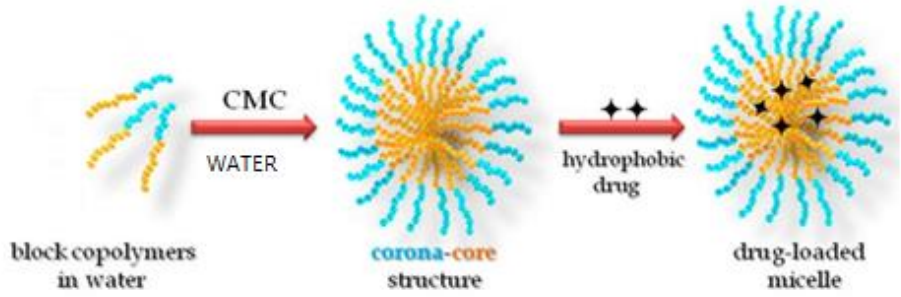

Fig. 1.3. Schematic of the micellization of diblock copolymers and the encapsulation of drug molecules [3].

1.3.3.1. Characteristics of the micelle morphology

The micelles' shell is made up of the hydrophilic blocks of amphiphilic copolymers. The charge, lipophilicity, and size of the micelles are all determined by the shell of the micellar structure. These parameters have a significant impact on carrier biological properties such as biocompatibility, pharmacokinetics, and blood circulation time [28]. The micellar morphology is influenced by a number of factors. The CMC, packing parameter, and aggregation number are the most critical components. Micelle formation in aqueous solution is fueled by hydrophobic interactions between the copolymer's hydrophobic blocks and the solvent. The size of the micelles and their drug loading capacity are substantially influenced by the balance between the hydrophobic and hydrophilic sections of the copolymers. Increased hydrophobicity results in a decreased CMC, which aids micelle formation and produces more stable micelles [29]. The CMC is primarily determined by the hydrophobic and hydrophilic ratios, as well as polymer-solvent interactions, which can be changed by variables such as solution temperature and pH. The packing parameter is the most important

component that determines the morphology of micelles. The packing parameter has the following definition:

$$p = \frac{v}{a_0 * l_c}$$

where a0 is the hydrophilic group's contact area, and lc and v are the length and volume of the hydrophobic block, respectively. Spherical micelles are created for p<1/3, cylinders are formed for 1/3p>1/2, and vesicles are formed for 1/2>p1 [30].

The aggregation number is the number of polymer chains that combine to create a micelle. The aggregation number is highly influenced by the copolymer's chain length and the ratio of hydrophobic to hydrophilic segments [31].

1.4. Mechanisms of drug release from polymeric micelles

The transportation of a drug molecule from the polymeric micelle to its exterior and into the surrounding environment is referred to as drug release [32]. The primary drug release mechanisms are shown in **Fig. 1.4**: polymer degradation, passive diffusion of encapsulated molecules, and a combination of the two [33]. The degradation of the polymeric chains causes the micelles to destabilize, allowing the medication to escape (**Fig. 1.4a**). The drug molecules simply diffuse through the micelle and into the surrounding media as seen in **Fig. 1.4b**. Finally, in **Fig. 1.4c**, we can see the release caused by a combination of diffusion and polymer degradation. The drug's release mechanism can be separated into two phases: in phase 1, drug molecules diffuse fast into the medium as a result of drug absorption onto the nanocarriers' surface. This phase is known as the burst release phase. The process of release in phase 2 (controlled release phase) is determined by the properties of the polymeric system. When the rate of drug diffusion is larger than the rate of polymer degradation, diffusion is the major process; otherwise, polymer degradation is the driving force of drug release [34].

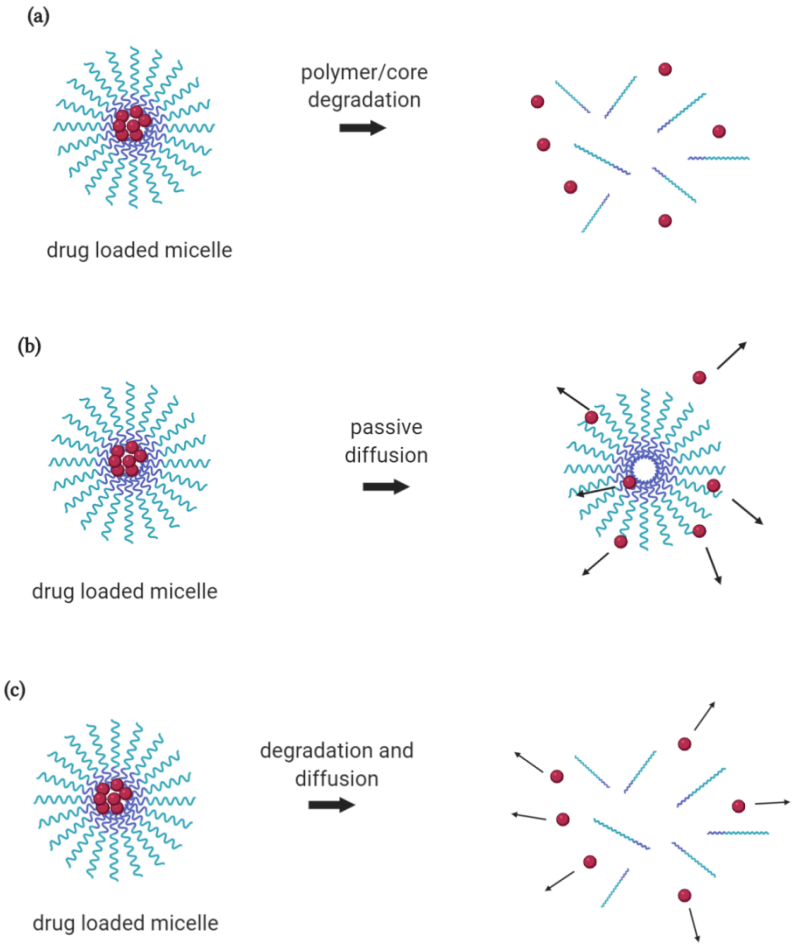

Fig. 1.4. Schematic of release mechanisms from drug loaded micelles by a) degradation of the polymeric chains, b) diffusion of the drug molecules c) a combination of degradation and diffusion. Created with BioRender.com

1.4.1. Factors affecting drug release

Drug release from polymeric micelles is influenced by a variety of factors. The higher the molecular weight, the larger the size of the micelles which slows down the release rate. The length of the copolymer's hydrophilic and hydrophobic blocks has a significant impact on drug molecule release. The larger the micelle core (the longer the hydrophobic chain), the greater the drug loading capacity [22].*Yang et al.* found that copolymers with longer PLA chains produce closely packed micelles as a result of hydrophobic interactions between drug molecules and PLA chains, resulting in a slower drug release rate from the micelles [35]. Finally, the size, shape, drug loading capacity, and stability of nanocarriers, as well as the rate

and degree of drug release, can be influenced by the micelle manufacturing procedure [36].The concentration of the copolymer, the pH of the solution, and the solvent are all critical aspects in drug release [37].

1.5. Ring Opening Polymerization (ROP)

Ring opening polymerization, according to IUPAC, is a method of polymerizing cyclic monomers to produce acyclic or polymers with fewer cycles [38]. A reactive center in a polymer chain attacks a cyclic monomer, forming an acyclic chain and initiating the polymerization of the next monomer. The active polymeric chain can be anionic, cationic or radical. This technique has several advantages, including the capacity to produce high molecular weight polymers with a regulated polydispersity index (PDI) [39]. Catalysts are required for ROP to proceed. Metal –catalysts, such as lead, aluminum, zinc, yttrium, and bismuth salts, have been employed in the industrial production of PLLA. Tin(II) 2-ethylhexanoate or stannous octoate ($Sn(Oct)_2$) are the most often used metal-complexes.
Figure. 1.5 illustrates the general scheme of ring-opening polymerization.

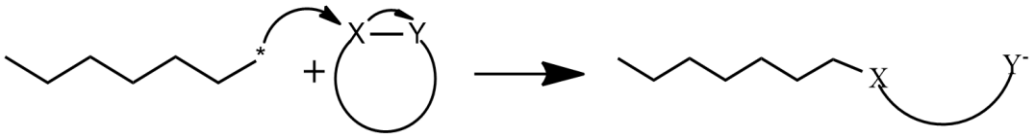

Fig. 1.5. General scheme of ROP. The * refers to anionic, cationic or radical chain.

1.6. Flurbiprofen

Flurbiprofen (2-(3-fluoro-4-phenylphenyl)propanoic acid), a propionic acid derivative, is an antipyretic and analgesic nonsteroidal anti-inflammatory drug (NSAID) (**Fig.1.6.**). Flurbiprofen oral formulations can be used to treat the symptoms of rheumatoid arthritis, osteoarthritis, and anklylosing spondylitis. Flurbiprofen can also be used topically to prevent or minimize intraoperative miosis prior to ocular surgery. Fenoprofen, ibuprofen, and ketoprofen are structurally and pharmacologically linked to flurbiprofen [40].

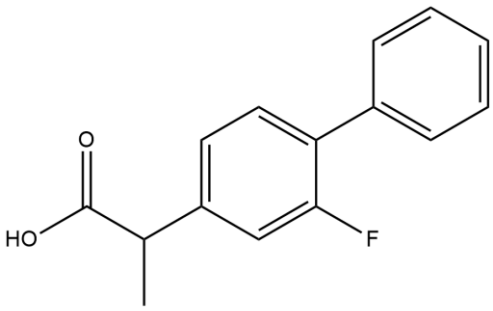

Fig.1.6. Structure of Flurbiprofen

Chapter 2: Research methodology

2.1. Materials

Poly(ethylene glycol) methyl ether (MePEG) with molecular weight of 5000 gr/mol was purchased from Polysciences Inc. PEG with 4000 gr/mol molecular weight was purchased from Sigma-Aldrich. L-lactide and stannous octoate (95%) as the catalyst were obtained from Sigma-Aldrich. Flurbiprofen was gifted from the School of Medicine, University of Crete. Tetrahydrofuran (THF) (HPLC grade ≥ 99.9%), methanol and petroleum ether were purchased from Scharlau S. L. THF was purchased from Carlo Erba Reagents and deuterated chloroform (≥ 99.8%) was obtained from Deutero GmbH. Finally, dichloromethane (≥ 99.9%), 2-propanol (≥99.5%) and toluene (≥ 99.9%) were purchased from Sigma-Aldrich. Milli-Q water with a resistivity of 18.2 MΩ.cm at 298 K was obtained from a Millipore apparatus and was used for all the experiments.

2.2. Synthesis of poly(ethylene-glycol) methyl ether-*b*-poly(L-lactide) (MePEG-*b*-PLLA) diblock copolymers and PLLA-*b*-PEG-*b*-PLLA triblock copolymers

The synthesis of MePEG-*b*-PLLA copolymer was achieved through a ring-opening polymerization of L-lactide using MePEG as the initiator and $Sn(Oct)_2$ as the catalyst. Briefly, freeze-dried MePEG (0.33gr, 7.6 mmol), recrystallized L-lactide (1gr, 13.9 mmol) and the catalyst (1%), were added into the reaction vessel. Right after, the reaction was purched with N_2 for 30 min and then it was placed in an oil bath at 130 °C for 24 hours under stirring.. Afterwards, the final product was dissolved in dichloromethane and was precipitated in petroleum ether.The supernatant was disposed and the product was left under vacuum to dry.

The same procedure was followed for the synthesis of the PLLA-*b*-PEG-*b*-PLLA triblock copolymer with bifunctional PEG instead of monofunctional MePEG .More specific,freeze-dried PEG (0.4gr, 9mmol), recrystallized L-lactide (1gr, 13.9mmol) and the catalyst (1%) were placed into the vessel,purged under N_2 for 30 min and placed in the oil bath at 130°C for 24 hours under stirring. Dichloromethane was used to dissolve the final product, which was then precipitated in petroleum ether.

The precipitated polymers were characterized by SEC and ^{1}H NMR spectroscopy.

2.3. Preparation of the PEG-*b*-PLLA and PLLA-*b*-PEG-*b*-PLLA nanocarriers

The nanocarriers were prepared with the non-selective-selective solvent dissolution method. Briefly, 20 mg of the polymer - diblock or triblock copolymer- were dissolved in 2.5 ml of THF. Then 15 ml of milli-Q water (pH 7.4) were added using a syringe pump at a rate of 0.05 ml/min. Next, the organic solvent was evaporated under vacuum using a rotary evaporator. Finally, the solution was filtered through a hydrophilic Chromapure PVDF/L filter with 0.45 μm pore size and was stored in the fridge until use. Nanocarriers consisted from both the diblock MePEG-*b*-PLLA and the triblock PLLA-*b*-PEG-*b*-PLLA were also prepared by mixing equal amounts of the polymers and following the same procedure. The size of the nanocarriers was determined by dynamic light scattering (DLS) and their shape and

morphology were confirmed by field emission scanning electron microscopy (FESEM) and transmittance electron microscopy (TEM), respectively.

2.4. Preparation of Flurbiprofen loaded PEG-*b*-PLLA and PLLA-*b*-PEG-*b*-PLLA nanocarriers

A stock solution of the drug with concentration 1 mg/ml was prepared in THF. The encapsulation of the Flurbiprofen was achieved using the non-selective-selective solvent dissolution technique. Briefly, 20 mg of the polymer - diblock or triblock copolymer- were dissolved in 2.5 ml of THF and afterwards, 400 μl of stock solution were added in the polymer solution and the same procedure as that described above for the polymeric micelles was followed. Also micelles loaded with Flurbiprofen from both of the copolymers were prepared by dissolving 10 mg of each polymer in 2.5 ml of THF and adding 400μl of the Flurbiprofen stock solution. The procedure was carried out as before.

2.5. Release studies methodology of Flurbiprofen

To study the release profile of the drug from the polymeric nanocarriers, 4 ml of the prepared micellar solutions were transferred into a dialysis membrane with MWCO of 3.500. The dialysis membrane was then placed in a vial and 40 ml of milli-Q water with pH 7.4 were added. The vial then was placed in a water bath at constant temperature of 37°C to simulate the body temperature. At predetermined time intervals, the water medium was taken out of the vial and it was replaced with fresh water. The collected samples were evaporated under vacuum. The dried samples were dissolved in 3 ml of isopropanol and released Flurbiprofen was determined by fluorescence spectroscopy using a calibration curve of Flurbiprofen in isopropanol.

2.6. Characterization methods

2.6.1. Size Exclusion Chromatography (SEC)

In order to determine the molecular weights and the PDIs of the polymers, SEC was used, equipped with a Waters-515 isocratic pump, two columns, Mixed-D and Mixed-E (Polymer

Labs), a Waters 2745 Dual Absorbance detector and a Waters 410 refractive index (RI) detector. THF (HPLC grade) with 2% v/v TEA was used as the eluent at a flow of 1 ml/min and the column temperature was set at 25 C. Usually 20-30 mg of the polymer were dissolved in 1 ml THF (HPLC). Next, the solution was filtered through a PTFE filter with 0.45 μm pore size and was consequently injected into the system. The molecular weight of the polymer was calculated using a calibration curve based on PMMA standards with molecular weights ranging from 625-138600 gr/mol.

2.6.2. Proton Nuclear Magnetic Resonance (^{1}H NMR) spectroscopy

The polymers were characterized by ^{1}H NMR spectroscopy on an Avance Bruker 300 MHz spectrometer with tetramethylsilane (TMS) as an internal standard and $CDCl_3$ as the solvent.

2.6.3. Field emission scanning electron microscopy (FE-SEM)

FESEM images were obtained using a JEOLJSM-7000F microscope. A drop of the sample was deposited on a glass panel and was left to dry overnight at room temperature. Then the sample was sputter-coated with Au (10mm thick) before imaging.

2.6.4. Dynamic Light Scattering (DLS)

The size of the micelles was measured using a Malvern Zetasizer Nano ZS instrument equipped with a 4 MW He-Ne laser operating at λ = 632.8 nm. The scattering angle was 90° and three scans were collected for each measurement.

2.6.5. Transmission Electron Microscopy (TEM)

TEM images were captured with a JEOL JEM-2100 instrument at 80 KV. A drop of the sample was deposited on a carbon-coated cooper grid and was left to dry overnight

.

2.6.6. Fluorescence spectroscopy

The fluorescence spectra were recorded using a Lumina Fluorescence Spectrometer by Thermo Fisher Scientific. The excitation and emission wavelengths were set at 248 and 260 nm, respectively. The emission and excitation slits were both set to 5 nm and 20 nm. The response time was set at 2 s. The samples were measured in quartz cuvettes

Chapter 3: Results and Discussion

3.1 Synthesis and characterization of PEG-*b*-PLLA diblock and PLLA-*b*-PEG-*b*-PLLA triblock copolymers

As mentioned before, the ring-opening polymerization was used to synthesize PEG-*b*-PLLA diblock and PLLA-*b*-PEG-*b*-PLLA triblock copolymers. The synthesis of the PEG-*b*-PLLA diblock copolymer is shown schematically in **Fig. 3.1a**, whereas the synthesis of the triblock copolymers is shown schematically in **Fig. 3.1b.** PEG was used as an initiator in the polymerization of the monomer, L-lactide. The polymerization of the diblock copolymer begins at the hydroxyl group of MePEG. A bifunctional PEG was used in the case of the triblock. PEG's hydroxyl groups on both ends worked as initiators, and L-lactide polymerization began on both sides.

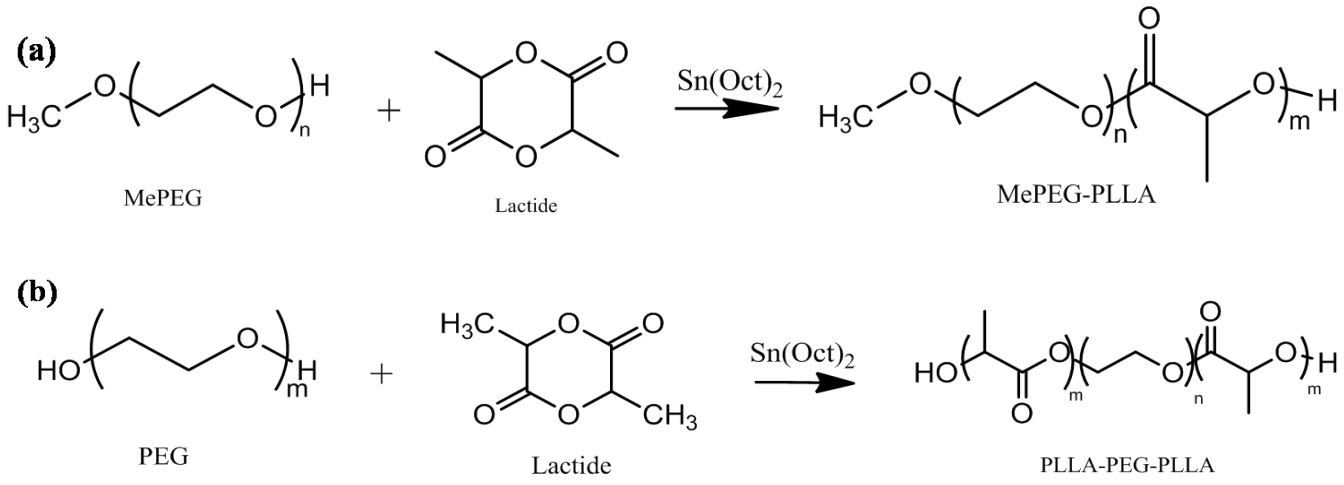

Fig. 3.1. Synthesis of (a) PEG-*b*-PLLA diblock copolymer and (b) PLLA-*b*-PEG-*b*-PLLA triblock copolymer.

The successful synthesis of the copolymers was confirmed by SEC. The molecular weight of the PEG-*b*-PLLA diblock copolymer was found 26551 g/mol with a PDI 1.41. On the other hand the molecular weight of the PLLA-*b*-PEG- *b*-PLLA triblock copolymer was found 14074 g/mol with a PDI 1.33. The chromatogram of the diblock copolymer is shown in **Figure 3.2a.**, whereas the chromatogram of the PLLA-b-PEG- b-PLLA triblock copolymer is shown in **Figure 3.2b**. As it is observed, the SEC peak of the MePEG is appeared at elution time 14.1 min while the copolymer peak is appeared at 13.3 min. The appearance of the copolymer peak at lower elution times and thus higher molecular weight indicates the successful polymerization of the lactide monomer from the PEG macroinitiator. Similarly, for the triblock copolymer, the SEC peak of the PEG block is appeared at elution time 15 min while the copolymer peak is appeared at lower elution time 13.3 min, again showing the successful polymerization. The SEC curves of the block copolymers and the PEG macroinitiators slightly overlap, indicating the existence of PLLA homopolymer. As it has already discussed, ROP can start from hydroxyl groups, thus traces of water molecules in the reaction could also start the polymerization resulting in the production of PLLA homopolymers which is difficult to separate from the block copolymer chains.

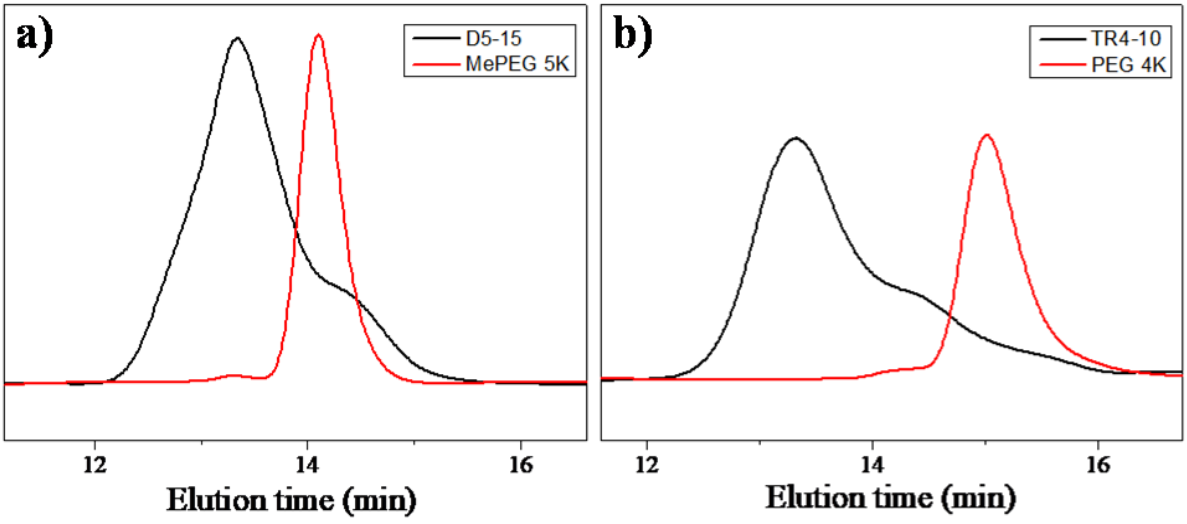

Fig. 3.2. SEC traces of (a) D5-15 diblock copolymer and (b) TR4-10 triblock copolymer.

The chemical structure and the composition of the diblock and triblock copolymers were determined by ^{1}H NMR spectroscopy. **Fig. 3.3a.** shows the ^{1}H NMR spectrum of the diblock copolymer.

The peak at 1.6 ppm (a) is assigned to the methyl protons of the L-lactide monomer repeating unit, the peak at 5.18 ppm (b) refers to the proton of the –CH group of the lactide units, while the peak at 3.66 ppm (c) is assigned to the CH_2 protons of the PEG block. Similar, for the triblock copolymer, the peak of the methyl group of the L-lactide monomer repeat units at 1.58 ppm (a), the peak of the proton of the –CH group of the lactide units at 5.19 ppm (b), and the 4 protons of PEG at 3.66 ppm (c), are observed (**Fig. 3.3b.**). We can calculate the number of protons assigned to PLLA and hence determine the molecular weight of the diblock and triblock copolymers by determining the number of hydrogen atoms in the product that are assigned to PEG and integrating the appropriate peaks.

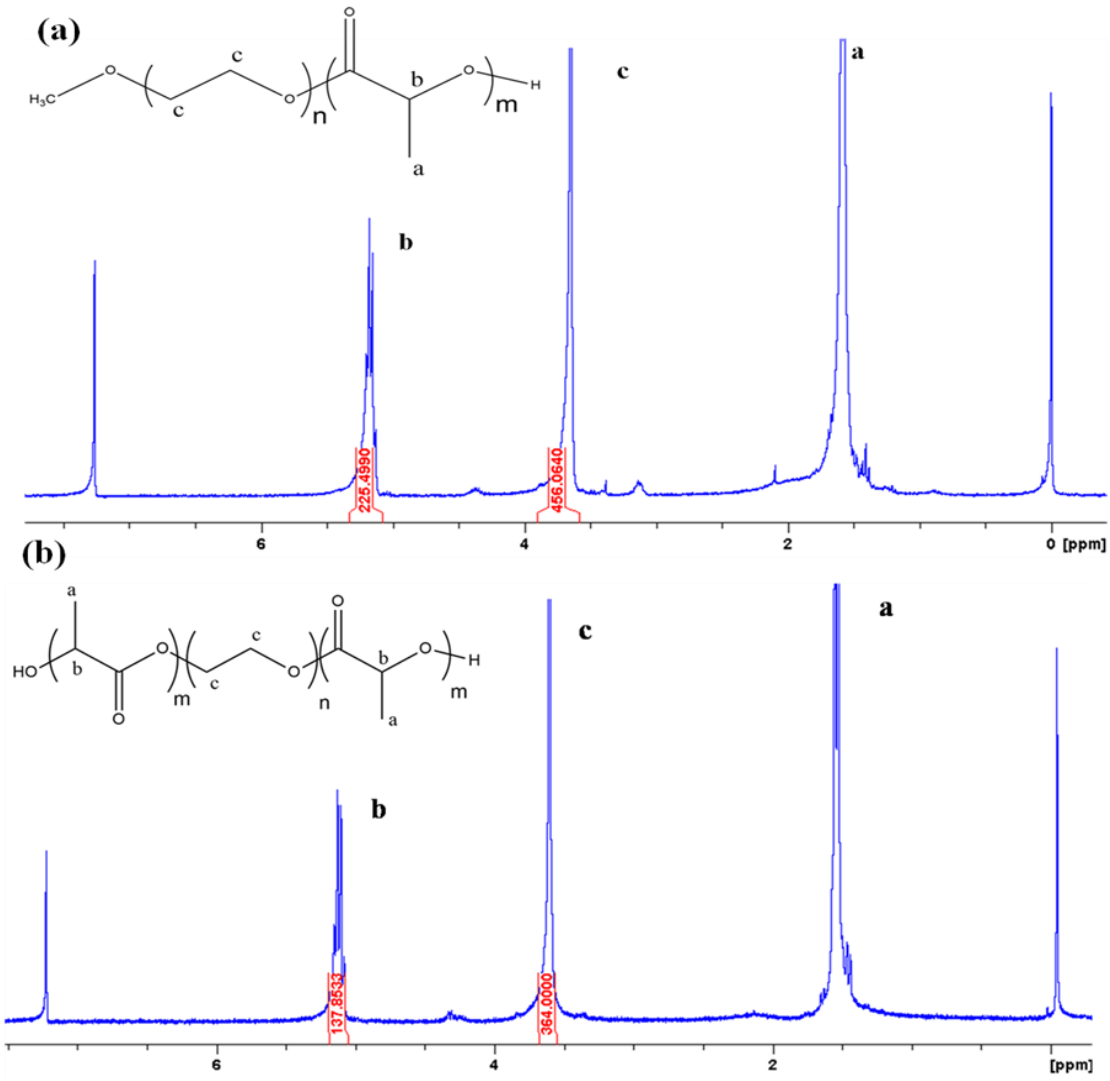

Fig. 3.3 : ^{1}H NMR spectra of a) diblock and b) triblock copolymer

Table 3.1. summarizes the molecular weights, degree of polymerization, polydispersity index (PDI) as well as the conversion percentage of the synthesized polymers.

Table 3.1. Characterization of diblock and triblock copolymer by SEC and ^{1}H NMR

Polymer	DP_{PEG}	$DP_{PLLA,th}$	$DP_{PLLA,NMR}$	Mn_{NMR}	Mn_{GPC}	Mn_{th}	PDI	Conv% (NMR)
D5-15	114	208	225	21200	26551	20000	1.38	97%
TR4-10	91	138	138	13900	14074	14000	1.57	99%

3.2. Self-assembly of the PEG-*b*-PLLA and PLLA-*b*-PEG-*b*-PLLA diblock and triblock copolymers.

The ability of the amphiphilic copolymers to self-assemble into nanosized structures was investigated. The non-selective-selective solvent approach was followed to prepare the nanocarriers. It is known that this method produces micelles with uniform size and low PDI. In the case of the diblock, the average size of the micelles was 133 nm as shown in **Fig. 3.4a**. FESEM and TEM (**Fig. 3.4b and Fig. 3.4.c**) confirmed the spherical shape of the micelles and their size from FESEM was found to be 55 nm. The smaller size acquired from FESEM is due to the dry nature of the technique and the collapse of the micellar corona.

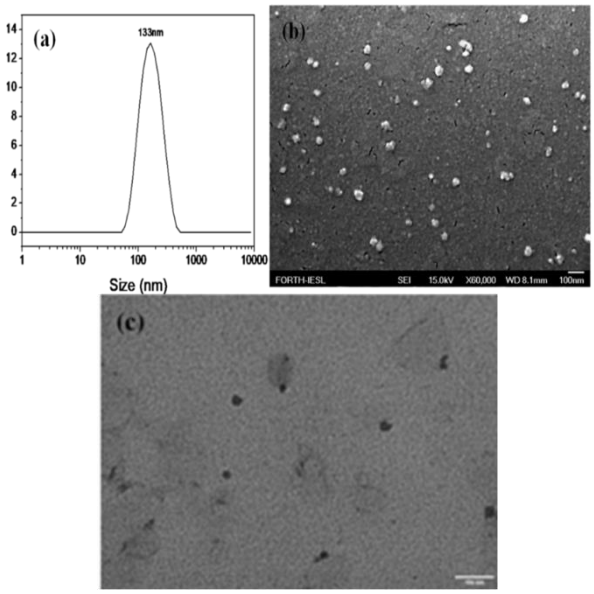

Fig. 3.4. a) DLS measurment of D5-15 copolymer micelles b) FE-SEM image of D5-15 copolymer micelles (scale bar, 100nm) c) TEM image of D5-15 copolymer micelles (scale bar,100nm) .

The triblock copolymer also formed nanostructures with a mean size of 177 nm (**Fig. 3.5a**) and their spherical morphology was established by FESEM as shown in **Fig. 3.5b**. Once more the measured size from FESEM was found to be smaller than the size reported from the DLS experiment, at 98 nm, which again can be attributed to the preparation method of the samples.

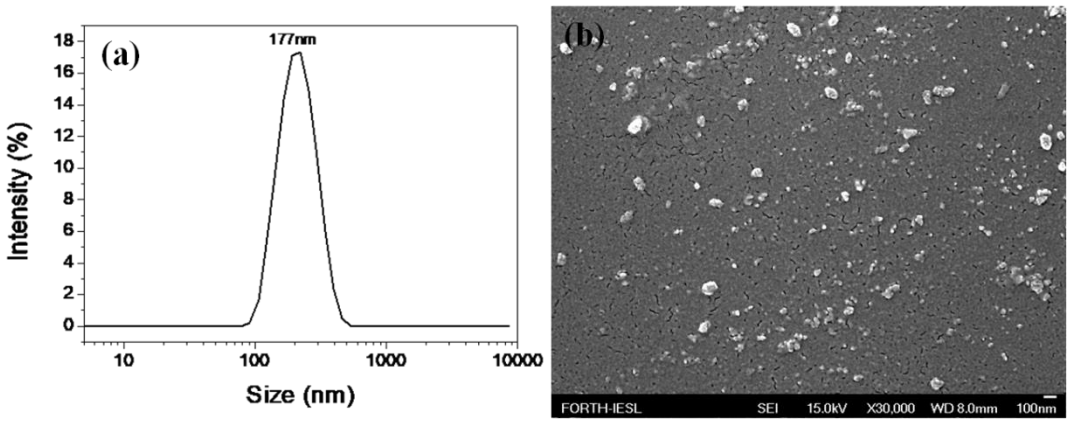

Fig. 3.5. a) DLS measurment of TR4-10 micelles b) FE-SEM image of TR4-10 micelles (scale bar,100nm).

In addition, the self-assembly behavior of a mixture of D5-15 and TR4-10 copolymers in order to obtain more complex structures of nanocarriers, was studied. Flurbiprofen was encapsulated into the nanocarriers and their morphological characteristics were studied. In this case two size distributions were observed in DLS. The first one at 33 nm and the second one at 198 nm (**Fig. 3.6a**).The size at 198 nm probably resulted from micellar aggregates. The obtained nanocarriers were spherical with a micellar structure as observed by FESEM (**Fig. 3.6b)** and TEM (**Fig. 36c)** microscopies. The size obtained from the FESEM was at 105 nm. The micelles appeared darker from TEM because of the loaded Flurbiprofen.

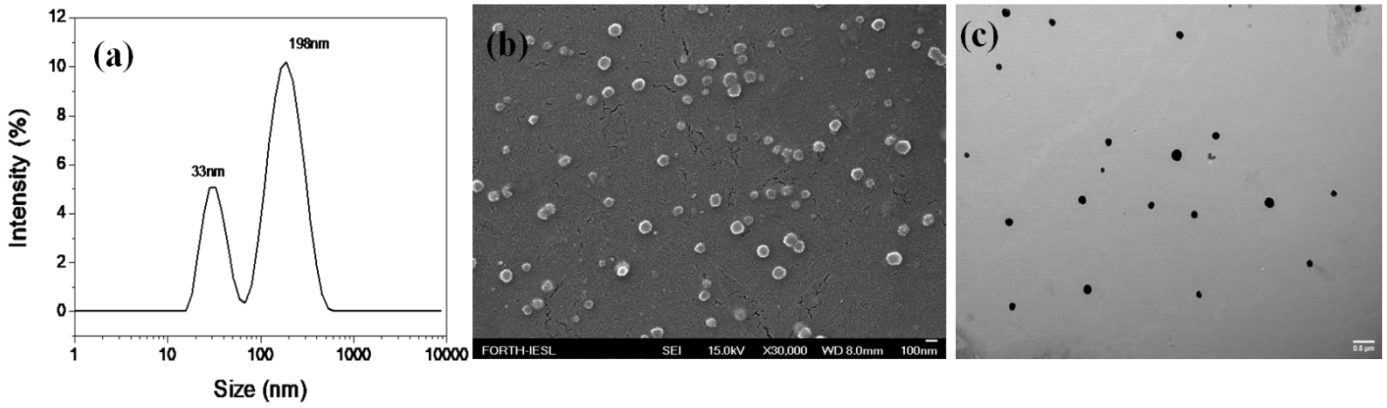

Fig. 3.6. a) DLS measurment of mixed copolymer micelles b) FE-SEM image of mixed copolymer micelles (scale bar, 100 nm) c) TEM image of mixed copolymer micelles (scale bar,0.5 μm).

3.3. Release Studies of Flurbiprofen

The previous results show the successful self-assembly of the diblock, triblock as well as the mixture of the di- and triblock and the formation of spherical nanostructures. Next, the release profile of the drug from the three formulations was examined. The release kinetics of Flurbiprofen from the polymeric nanocarriers is presented in **Figure 3.7.** First, the release profile of Flurbiprofen from the diblock copolymer micelles was investigated. The micelles had a maximum loading of 8 μg and approximately 90% of the drug was released during the first 24 h. This could be attributed to the passive diffusion of Flurbiprofen from the micelles into the aqueous medium. The system reached a plateau in about four days, as illustrated in **Fig 3.7**. Next, the release profile of Flurbiprofen from polymeric micelles of the TR4-10 triblock copolymer was investigated. As shown in **Fig. 3.7.**, the micelles were able to

encapsulate only 2.5 μg of the drug and released about 50% in the first 6 hours, while reaching a plateau in four days. The small loading capacity can be explained by the fact that the PLLA block of the triblock copolymer had lower molecular weight than the diblock, leading to the formation of a smaller hydrophobic core and thus to lower encapsulation efficiency. It is worth noting that despite the difference between the loading capacities, both of the polymeric micelles released the drug within four days.

The diblock and triblock copolymers were clearly incapable of loading a significant amount of Flurbiprofen or prolonging the drug's release duration on their own. To circumvent these challenges, we prepared mixed micelles out of the polymers **(Fig.3.7)**. This time, the polymeric micelles were able to encapsulate higher amount of drug (about 45 μg) and they released about 50% in four hours and almost 100% in about 7 days. It is obvious that the complex mixed micelles had a higher loading capacity and slower release of the drug molecules compared to the diblock and triblock polymeric micelles alone. Nevertheless, more research is needed to determine the release behaviour of mixed micelles and to better understand the mechanism that drives it.

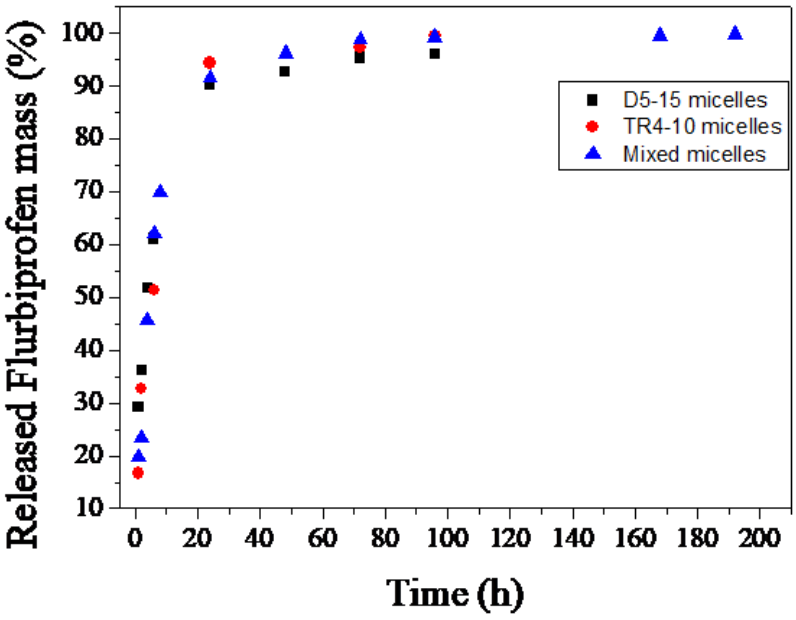

Fig. 3.7 : Flurbiprofen release from polymeric micelles of D5-15,TR4-10 and a mix of D5-15 and TR4-10.

Chapter 4: Conclusions and future perspectives

The intricate structure of the eye has made delivering drugs to the eye a difficult task for scientists. Liposomes, polymeric nanoparticles, polymeric micelles and vesicles, among other nanocarriers, have been employed in the past to efficiently carry medicinal compounds. As therapeutic carriers, polymeric micelles made up of biodegradable, amphiphilic block copolymers have been extensively utilized. The primary goal of this thesis was to create biodegradable diblock and triblock copolymers that could self-assemble into micellar structures for ocular drug delivery.

MePEG-*b*-PLLA and PLLA-*b*-PEG-*b*-PLLA copolymers were synthesized and studied using SEC and ^{1}H NMR spectroscopy. The non-selective-selective solvent dissolution method was used to achieve block copolymer self-assembly. DLS was used to determine the size of the nanocarriers, while FESEM and TEM were used to corroborate their morphology. Micelles with a diameter of 133 nm were formed by the diblock copolymer, while micelles with a diameter of 177 nm were formed by the triblock copolymer. Finally, the formation of mixed micelles from the two copolymers gave nanocarriers with sizes at 33 and 198 nm.

In order to examine the release kinetics of Flurbiprofen from the polymeric nanocarriers, the micelles were loaded with the drug and placed in a bath at 37°C to simulate the body temperature. The results showed that the micelles formed from the diblock copolymer released almost 8 μg of the drug and reached a steady state after 48 hours while the triblock polymeric micelles were able to release 100% of Flurbiprofen in about 4 days. To obtain even better loading amount and slower releasing rate, we also prepared more complex micelles from the combination of both the diblock and the triblock copolymers. This system was able to encapsulate 45 μg of the drug and release all of it in about 7 days.

Future research will focus on the medication release mechanism from nanocarriers and their application in ocular drug delivery. In addition, research is needed to improve loading capability and slow the release rate even more.

References

[1] A. Mandal, R. Bisht, I. D. Rupenthal, and A. K. Mitra, "Polymeric micelles for ocular drug delivery: From structural frameworks to recent preclinical studies," *J. Control. Release*, vol. 248, pp. 96–116, 2017, doi: 10.1016/j.jconrel.2017.01.012.

[2] C. Zhang, L. Liao, and S. Gong, "Microwave-assisted synthesis of PLLA-PEG-PLLA triblock copolymers," *Macromol. Rapid Commun.*, vol. 28, no. 4, pp. 422–427, 2007, doi: 10.1002/marc.200600709.

[3] Y. H. A. Hussein and M. Youssry, "Polymeric micelles of biodegradable diblock copolymers: Enhanced encapsulation of hydrophobic drugs," *Materials*. 2018, doi: 10.3390/ma11050688.

[4] K. K. Jain, "Drug delivery systems - An overview," *Methods Mol. Biol.*, vol. 437, pp. 1–50, 2008, doi: 10.1007/978-1-59745-210-6_1.

[5] S. S. Venkatraman, P. Jie, F. Min, B. Y. C. Freddy, and G. Leong-Huat, "Micelle-like nanoparticles of PLA-PEG-PLA triblock copolymer as chemotherapeutic carrier," *Int. J. Pharm.*, vol. 298, no. 1, pp. 219–232, 2005, doi: 10.1016/j.ijpharm.2005.03.023.

[6] C. H. Tsai, P. Y. Wang, I. C. Lin, H. Huang, G. S. Liu, and C. L. Tseng, "Ocular drug delivery: Role of degradable polymeric nanocarriers for ophthalmic application," *International Journal of Molecular Sciences*, vol. 19, no. 9. 2018, doi: 10.3390/ijms19092830.

[7] W. Gao, J. M. Chan, and O. C. Farokhzad, "PH-responsive nanoparticles for drug delivery," *Molecular Pharmaceutics*, vol. 7, no. 6. American Chemical Society, pp. 1913–1920, Dec. 06, 2010, doi: 10.1021/mp100253e.

[8] L. Zhang *et al.*, "Self-assembled lipid-polymer hybrid nanoparticles: A robust drug delivery platform," *ACS Nano*, vol. 2, no. 8, pp. 1696–1702, Aug. 2008, doi: 10.1021/nn800275r.

[9] S. Liu, L. Jones, and F. X. Gu, "Nanomaterials for Ocular Drug Delivery," *Macromol. Biosci.*, vol. 12, no. 5, pp. 608–620, May 2012, doi: 10.1002/mabi.201100419.

[10] E. M. del Amo, *Ocular and systemic pharmacokinetic models for drug discovery and development*. 2015.

[11] P. R. Karn, H. Do Kim, H. Kang, B. K. Sun, S. E. Jin, and S. J. Hwang, "Supercritical fluid-mediated liposomes containing cyclosporin A for the treatment of dry eye syndrome in a rabbit model: Comparative study with the conventional cyclosporin A emulsion," *Int. J. Nanomedicine*, 2014, doi: 10.2147/IJN.S65601.

[12] B. D. Ulery, L. S. Nair, and C. T. Laurencin, "Biomedical applications of biodegradable polymers," *Journal of Polymer Science, Part B: Polymer Physics*. 2011, doi: 10.1002/polb.22259.

[13] H. K. Makadia and S. J. Siesize, "Poly Lactic-co-Glycolic Acid (PLGA) as biodegradable controlled drug delivery carrier," *Polymers (Basel).*, 2011, doi: 10.3390/polym3031377.

[14] M. S. Muthu, "Nanoparticles based on PLGA and its co-polymer: An overview," *Asian J. Pharm.*, vol. 3, no. 4, pp. 266–273, 2009, doi: 10.4103/0973-8398.59948.

[15] C. Cañadas *et al.*, "In vitro, ex vivo and in vivo characterization of PLGA nanoparticles loading pranoprofen for ocular administration," *Int. J. Pharm.*, 2016, doi: 10.1016/j.ijpharm.2016.07.055.

[16] K. Nagpal, S. K. Singh, and D. N. Mishra, “Chitosan nanoparticles: A promising system in novel drug delivery,” *Chemical and Pharmaceutical Bulletin*. 2010, doi: 10.1248/cpb.58.1423.

[17] R. C. Nagarwal, P. N. Singh, S. Kant, P. Maiti, and J. K. Pandit, “Chitosan nanoparticles of 5-fluorouracil for ophthalmic delivery: Characterization, in-vitro and in-vivo study,” *Chem. Pharm. Bull.*, 2011, doi: 10.1248/cpb.59.272.

[18] N. C. Silva, S. Silva, B. Sarmento, and M. Pintado, “Chitosan nanoparticles for daptomycin delivery in ocular treatment of bacterial endophthalmitis,” *Drug Deliv.*, 2015, doi: 10.3109/10717544.2013.858195.

[19] S. Biswas, O. S. Vaze, S. Movassaghian, and V. P. Torchilin, “Polymeric Micelles for the Delivery of Poorly Soluble Drugs,” *Drug Deliv. Strateg. Poorly Water-Soluble Drugs*, pp. 411–476, 2013, doi: 10.1002/9781118444726.ch14.

[20] D. A. Chiappetta and A. Sosnik, “Poly(ethylene oxide)-poly(propylene oxide) block copolymer micelles as drug delivery agents: Improved hydrosolubility, stability and bioavailability of drugs,” *European Journal of Pharmaceutics and Biopharmaceutics*, vol. 66, no. 3. Elsevier, pp. 303–317, Jun. 01, 2007, doi: 10.1016/j.ejpb.2007.03.022.

[21] S. Fusco, A. Borzacchiello, and P. A. Netti, “Perspectives on: PEO-PPO-PEO Triblock Copolymers and their Biomedical Applications,” *J. Bioact. Compat. Polym.*, vol. 21, no. 2, pp. 149–164, Mar. 2006, doi: 10.1177/0883911506063207.

[22] I. G. Shin, S. Y. Kim, Y. M. Lee, C. S. Cho, and Y. K. Sung, “Methoxy poly(ethylene glycol)/ε-caprolactone amphiphilic block copolymeric micelle containing indomethacin. I. Preparation and characterization,” *J. Control. Release*, vol. 51, no. 1, pp. 1–11, Jan. 1998, doi: 10.1016/S0168-3659(97)00164-8.

[23] C. Allen, Y. Yu, D. Maysinger, and A. Eisenberg, “Polycaprolactone-b-poly(ethylene oxide) block copolymer micelles as a novel drug delivery vehicle for neurotrophic agents FK506 and L-685,818,” *Bioconjug. Chem.*, vol. 9, no. 5, pp. 564–572, Sep. 1998, doi: 10.1021/bc9702157.

[24] F. Chen, G. Yin, and X. Liao, “Preparation , characterization and in vitro release properties of morphine-loaded PLLA-PEG-PLLA microparticles via solution enhanced dispersion by supercritical fluids,” pp. 1693–1705, 2013, doi: 10.1007/s10856-013-4926-1.

[25] X. Deng, S. Zhou, X. Li, J. Zhao, and M. Yuan, “In vitro degradation and release profiles for poly-dl-lactide-poly(ethylene glycol) microspheres containing human serum albumin,” *J. Control. Release*, 2001, doi: 10.1016/S0168-3659(01)00210-3.

[26] H. Danafar, K. Rostamizadeh, S. Davaran, and M. Hamidi, “PLA-PEG-PLA copolymer-based polymersomes as nanocarriers for delivery of hydrophilic and hydrophobic drugs: Preparation and evaluation with atorvastatin and lisinopril,” *Drug Dev. Ind. Pharm.*, vol. 40, no. 10, pp. 1411–1420, 2014, doi: 10.3109/03639045.2013.828223.

[27] C. Mu *et al.*, “Solubilization of flurbiprofen into aptamer-modified PEG-PLA micelles for targeted delivery to brain-derived endothelial cells in vitro,” *J. Microencapsul.*, vol. 30, no. 7, pp. 701–708, 2013, doi: 10.3109/02652048.2013.778907.

[28] M. Imran, M. R. Shah, and Shafiullah, “Amphiphilic block copolymers–based micelles for drug delivery,” in *Design and Development of New Nanocarriers*, Elsevier Inc., 2018, pp. 365–400.

[29] W. Zhou, C. Li, Z. Wang, W. Zhang, and J. Liu, “Factors affecting the stability of drug-loaded polymeric micelles and strategies for improvement,” *J. Nanoparticle Res.*, vol. 18, no. 9, pp.

1–18, 2016, doi: 10.1007/s11051-016-3583-y.

[30] Y. Mai and A. Eisenberg, “Self-assembly of block copolymers,” *Chem. Soc. Rev.*, vol. 41, no. 18, pp. 5969–5985, Aug. 2012, doi: 10.1039/c2cs35115c.

[31] S. C. Owen, D. P. Y. Chan, and M. S. Shoichet, “Polymeric micelle stability,” *Nano Today*, vol. 7, pp. 53–65, 2012, doi: 10.1016/j.nantod.2012.01.002.

[32] K. E. Uhrich, S. M. Cannizzaro, R. S. Langer, and K. M. Shakesheff, “Polymeric Systems for Controlled Drug Release,” *Chem. Rev.*, vol. 99, no. 11, pp. 3181–3198, 1999, doi: 10.1021/cr940351u.

[33] R. Z. Xiao, Z. W. Zeng, G. L. Zhou, J. J. Wang, F. Z. Li, and A. M. Wang, “Recent advances in PEG-PLA block copolymer nanoparticles,” *Int. J. Nanomedicine*, vol. 5, no. 1, pp. 1057–1065, 2010, doi: 10.2147/IJN.S14912.

[34] T. Niwa, H. Takeuchi, T. Hino, N. Kunou, and Y. Kawashima, “Preparations of biodegradable nanospheres of water-soluble and insoluble drugs with D,L-lactide/glycolide copolymer by a novel spontaneous emulsification solvent diffusion method, and the drug release behavior,” *J. Control. Release*, 1993, doi: 10.1016/0168-3659(93)90097-O.

[35] Z. L. Yang, R. L. Xin, W. Y. Ke, and Y. Liu, “Amphotericin B-loaded poly(ethylene glycol)-poly(lactide) micelles: Preparation, freeze-drying, and in vitro release,” *J. Biomed. Mater. Res. - Part A*, 2008, doi: 10.1002/jbm.a.31504.

[36] Y. Luo, X. Yao, J. Yuan, T. Ding, and Q. Gao, “Preparation and drug controlled-release of polyion complex micelles as drug delivery systems,” *Colloids Surfaces B Biointerfaces*, vol. 68, no. 2, pp. 218–224, Feb. 2009, doi: 10.1016/j.colsurfb.2008.10.014.

[37] Y. Wang, P. Li, T. T. D. Tran, J. Zhang, and L. Kong, “Manufacturing techniques and surface engineering of polymer based nanoparticles for targeted drug delivery to cancer,” *Nanomaterials*, vol. 6, no. 2, 2016, doi: 10.3390/nano6020026.

[38] A. D. Jenkins, R. F. T. Stepto, P. Kratochvíl, and U. W. Suter, “Glossary of basic terms in polymer science (IUPAC Recommendations 1996),” *Pure Appl. Chem.*, vol. 68, no. 12, pp. 2287–2311, Jan. 1996, doi: 10.1351/pac199668122287.

[39] S. Metkar, V. Sathe, I. Rahman, B. Idage, and S. Idage, “Ring opening polymerization of lactide: kinetics and modeling,” *Chem. Eng. Commun.*, vol. 206, no. 9, pp. 1159–1167, 2019, doi: 10.1080/00986445.2018.1550395.

[40] “Flurbiprofen: Uses, Interactions, Mechanism of Action | DrugBank Online.” https://go.drugbank.com/drugs/DB00712 (accessed Feb. 22, 2022).

APPENDIX: Characterization Techniques.

1) Size Exclusion Chromatography (SEC)

Size exclusion chromatography (SEC), or gel permeation chromatography (GPC), is a well-known polymer separation method that allows determination of the polymer molecular characteristics, such as the average molecular weight and molecular weight distribution. In general, SEC is an important analytical tool used to evaluate the molecular characteristics of natural or synthetic polymers and proteins. A SEC instrument comprises a pump, a detector (e.g. UV or IR or both) and one, two or more separating columns. The columns or the stationary phase are filled with porous beads such as polystryrene sizes. The beads are made with a variety of pore sizes that span the range of the sizes of the macromolecules to be separated. The pump circulates solvent (mobile phase) through the size columns and swells the size material in the column. A small amount of diluted polymer solution in the same solvent as the mobile phase is injected in the flowing solvent entering the columns. As the polymer solution passes through the columns, the largest polymer particles are excluded from all, but the largest pores and elute from the column first. Right after, smaller polymer coils can pass through smaller pores and are excluded later from the columns. In this way, SEC separates the molecules by their size in solution, which is their hydrodynamic volume (V_h). After separation, the solution passes through the detectors used in the system and are analyzed, upon proper calibration with narrow molar mass distribution standards.

2) ^{1}H NMR spectroscopy

NMR spectroscopy is a very useful technique commonly employed for the determination of the chemical structure of chemical compounds. ^{1}H NMR and ^{13}C NMR are most commonly used for the characterization of materials. NMR is a spectroscopic technique allowing to observe local magnetic fields around atomic nuclei. The sample with the material is placed in a magnetic field and the NMR signal is produced by excitation of the nuclei of the sample with radiowaves into nuclear magnetic resonance, which is detected with sensitive radio receivers. The signal provides the required information regarding the environment of the nuclei. The exact field strength (in ppm) of a nucleus comes into resonance relative to a reference standard, usually the signal of the deuterated solvent used. Electron clouds shield the nuclei from the external magnetic field causing them to absorb at higher energy (lower

ppm), while the neighboring functional groups “deshield” the nuclei causing them to absorb at lower energy (higher ppm). Chemically and magnetically equivalent nuclei resonate at the same energy and give a single signal or pattern. Protons on adjacent carbons interact and split each other’s resonances into multiple peaks following the n+1 rule with coupling constant J. Spin-spin coupling is commonly observed between nuclei that are one, two and three bonds apart. The area under an NMR peak is proportional to the number of nuclei that give rise to that resonance, thus by integration, the protons of that resonance can be calculated

3) Dynamic Light Scattering (DLS)

Light scattering is a powerful tool for the characterization of the size of polymer nanoparticles in solution. The monochromatic, coherent laser beam hits the particles, and is scattered, due to the Brownian motion of the particles that changes their distance in the solution, and a time-dependent fluctuation of the scattering intensity is observed. By changing the observation angle (θ) and thus the scattering vector (q) a measure of the particle size is provided. The form factor, that is the interference pattern of the scattered light, is characteristic of the size and shape of the scatterers. The larger the particles are the slower their Brownian motion. Accuracy and stability of the temperature during the entire measurement is essential since the viscosity of the liquid is related to the temperature.

The velocity of the Brownian motion is defined by the translational diffusion coefficient (D). The Stocks-Einstein equation is used to calculate the particles’ size based on the translational diffusion coefficient:

$$R_h = \frac{K_B T}{6\eta\pi D}$$

Where, (R_h) is the hydrodynamic radius, (η) is the viscosity of the solvent, (K_B) is the Boltzmann constant and (T) is the temperature.

4) Field Emission Scanning Electron Microscopy (FESEM)

Scanning electron microscopy is designed to provide high-resolution images of a sample placed on a surface. A tungsten filament emits electrons, which are focused by an electron optical system. The electron beam can scan the sample surface and can provide its composition at a point, along a line or over a rectangular area, by scanning the beam across the surface in a series of parallel lines. The sample is mounted on a stage that can be accurately moved in all three directions (x, y and z), normal to the plane of the sample. The instrument generally operates under high vacuum in a very dry environment in order to produce the high energy beam of electrons needed for imaging. However, most specimens destined for study in the SEM are poor conductors. In SEM, the imaging system depends on the specimen being sufficiently electrically conductive to ensure that the bulk of the incoming electrons go to ground. The formation of the image depends on the collection of the different signals that are scattered as a consequence of the high electron beam interacting with the sample. The two principal signals used to form images are backscattered and secondary electrons generated within the primary beam-sample interactive volume. The backscattered electron coefficient increases with increasing the atomic number of the specimen, whereas the secondary electron coefficient is relatively insensitive to the atomic number. This fundamental difference in the two signals has an important effect on the way samples may need to be prepared. The use of scanning electron microscopy may be considered when being able to interpret the information obtained from the SEM, and attempt to relate the form and structure of the two-dimensional images and the identity, validity and location of the chemical data, back to the three-dimensional sample from which the information was derived. The biggest difference between a FESEM and a SEM lies in the electron generation system. As the source of electrons, FESEM uses a field emission gun that provides extremely focused, high- and low-energy electron beams, which greatly improves spatial resolution and enables work to be carried out at very low potentials (0.02–5 KV). This helps to minimize the charging effect on non-conductive specimens and to avoid damage from the electron beam on sensitive samples.

5) Transmission Electron Microscopy (TEM)

In TEM, the beam of electrons from the electron gun is focused into a small, thin, coherent beam by the use of the condenser lens. This beam is restricted by the condenser aperture, which excludes high angle electrons. The beam then strikes the specimen, and electrons are transmitted depending upon the thickness and electron transparency of the specimen. The transmitted portion is focused by the objective lens forming an image on a phosphor screen or a charge coupled device (CCD) camera. Optional objective apertures can be used to enhance the contrast by blocking out high-angle diffracted electrons. The darker areas of the image represent the areas of the sample where fewer electrons are transmitted, while the lighter areas of the image represent the areas of the sample where electrons were transmitted through.

6) Fluorescence spectroscopy

The technique of fluorescence spectroscopy is based on the phenomenon of fluorescence, ie the emission of radiation from an excited molecule. In general, when a molecule in the ground state of energy interacts with radiation of appropriate frequency, the molecule absorbs the radiated energy and is excited, that is, it transitions to a higher energy level. This excitation is maintained for a short time, as the molecule eliminates the absorbed energy either in the form of heat or through radiation emission and returns to the ground state. The de-excitaton of the molecule through radiation emission is called photoluminescence and when it occurs in a short time (10^{-9}-10^{-6}s) from the moment of stimulation, it is characterized as fluorescence.

In more detail the fluorescence phenomenon can be described as a three-step process. In the first stage, an energy photon supplied by an external radiation source is absorbed by the molecule in the ground state. The result of this absorption is the transition of an electron from the ground state to the first excited electron simple state. Each electronic state is separated into individual vibrational levels and the transition usually takes place to the highest energy vibrational level of the first excited state. In the second stage, during the life of the excited state, the molecule loses energy due to changes in its configuration or collisions with molecules in its environment.

The loss of this energy leads to the transition of the electron from the highest to the lowest vibrational level of the first excited state and this process is called vibrational relaxation. Finally, in the third stage, the de-excitation of the molecule takes place, ie the transition of the electron from the lowest energy vibrational state of the state to the ground state with parallel emission of energy radiation.